Adenosine Reagentless Electrochemical Aptasensor Using a Phosphorothioate Immobilization Strategy

Helena Ceretti,[a] *Belén Ponce*,[a] *Silvana A. Ramírez*,[a] *Javier M. Montserrat*,[a,b]*

[a] Instituto de Ciencias, Universidad Nacional de Gral. Sarmiento, J. M. Gutierrez 1150, Los Polvorines (B1613GSX), Prov. de Bs. As., Argentina
[b] INGEBI (CONICET), Vuelta de Obligado 2490 (1428), Buenos Aires, Argentina
*e-mail: jmontser@ungs.edu.ar

Received: May 21, 2009
Accepted: August 22, 2009

Abstract
This work deals with the characterization of a phosphorothioate anchoring strategy for aptamer molecules linked to gold, in the context of electrochemical sensors, using adenosine aptamer as model system. Surface density of immobilized phosphorothioate oligonucleotide sequences has been explored for a range of oligonucleotide concentrations (0.055 – 55 μM), finding a consequent variation of molecular surface density ($3.5 \times 10^{11} - 2.8 \times 10^{13}$ molecules/cm^2). Most suitable aptamer concentration for adenosine recognition was also explored and found to be around 5.5 μM. As proof of concept of phosphorothioate strategy, electrochemical response to adenosine concentration was measured using a ferrocene-labeled oligonucleotide sequence, and phosphorothioate anchoring thermal stability was compared to thiol immobilization.

Keywords: Aptamers, Phosphorothioate, Electrochemical, Gold, Adenosine

DOI: 10.1002/elan.200900279

Electrochemical aptamer based (E-AB) sensors have emerged as a promising analytical alternative for a variety of targets, ranging from proteins to small organic molecules, in different application contexts [1, 2]. They are based on the molecular recognition capabilities of DNA or RNA aptamer sequences [3], obtained by SELEX methodologies [4]. The binding of the target molecule to the aptamer induces a folding transition from a random coil like conformation to a quite well defined structure [5]. This conformational switch has been used to translate the recognition event into the direct measurement of an electrochemical response. Using these principles, different electrode-aptamer architectures have been conceived [6], most of them using gold as substrate. All constructions share the common characteristic of having a sulfur anchoring point to gold surface [7], via a thiol modification on one of the oligonucleotide termini. This DNA immobilization strategy has been characterized by Tarlov [8 – 10] and others [11, 12], who studied the dependence of molecular surface density and non-specific binding on critical parameters. This well described Au-S link has been used as standard anchoring strategy for many biosensors developed so far. In the case of reagentless E-AB sensors, the redox label and the anchoring thiol are both on the same strand, which demands chemical modifications at 3′ and 5′ termini.

In this regard, an alternative to thiol anchoring could be the use of phosphorothioate linkages. This modification has been originally developed to render the internucleotide linkage resistance to nuclease degradation in biological fluids [13]. It has several advantages over thiol modification: it can be introduced in the same way at 3′-, 5′- or inner positions; does not require chemical activation prior to use, has low cost and can be simply synthesized in the oligonucleotide solid phase cycle using the Beaucage reagent [14]. Although the widespread application in antisense oligonucleotides, Au-phosphorothioate immobilization was only reported for a few genosensors [15, 16] and as linker in the assembling of gold nanoparticules [17, 18]. In any case, no characterization of the phosphorothioate immobilization was described, and no evidence was set that an E-AB sensor would properly function with this kind of anchoring.

In this work we explored the performance of an E-AB sensor targeting adenosine, using the aptamer sequence developed by Szostak [19]. Immobilization was performed via phosphorothioate as linker to gold, evaluating the modified oligonucleotide surface density and the electrochemical response to adenosine of a ferrocene-labeled aptamer oligonucleotide.

As a preliminary experiment, aptamer 1 was immobilized on a gold electrode and exploratory CV experiments were performed immersing the electrode in a 0.02 M $K_3[Fe(CN)_6]$ aqueous solution (Figure 1A). Compared to a bare gold surface, an apparent decrease in the magnitude of the anodic and cathodic currents and charges was observed. Also a negative potential shift for the peak potential (E_p) of the reduction process was experienced, while a positive shift in E_p was verified for the oxidation process in the curve corresponding to aptamer 1 immobilization. After treatment with

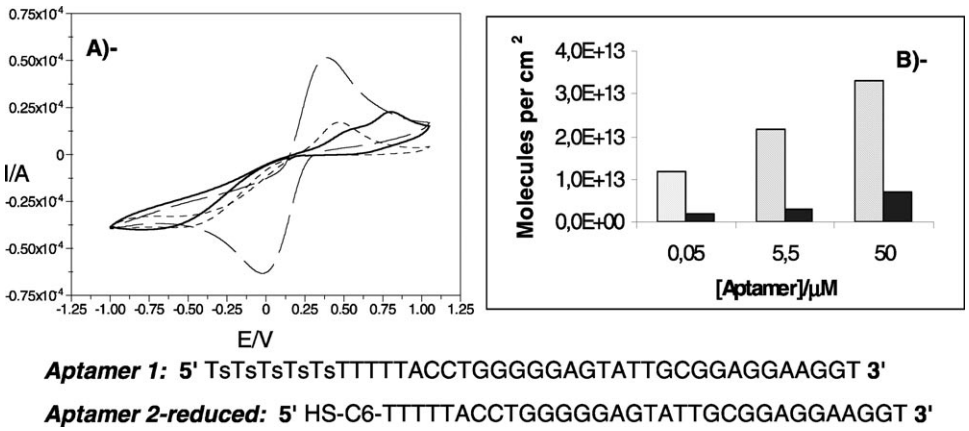

Fig. 1. A) CV of bare Au (– – –), Au + Aptamer 1 (——), Au + Aptamer 1 + MCH (-----). B) Electrode coverage by Aptamer 1 (black column) and Aptamer 2-reduced (grey column).

MCH, which is normally used as spacer [8], a new CV was registered showing a slight decrease in the magnitude of the current response. In both cases, before and after MCH treatment of aptamer 1 modified gold surface, the smaller currents due to oxidation of $[Fe(CN)_6]^{4-}$ and reduction of $[Fe(CN)_6]^{3-}$ appeared with an overpotential. This behavior has been reported in DNA and DNA/MCH modified electrodes and explained by repulsive electrostatic interactions that inhibit $[Fe(CN)_6]^{3-}$ from reaching the electrode surface [20, 21]. Thus, the voltammetric reversibility of $[Fe(CN)_6]^{3-}$ has been influenced by the interaction with the polyanionic layer of the immobilized aptamer.

Chronocoulometric experiments, in the presence of 50 μM $[Ru(NH_3)_6]^{3+}$ [10], were used to determine molecular surface density of aptamers 1 and 2. Comparison was made for three oligonucleotide concentrations (Fig. 1B), prior disulfide reduction in the case of aptamer 2. Immobilization via a thiol group is between five to ten times greater than anchoring via phosphorothioate, as shown by the number of aptamer molecules per cm^2.

In order to estimate the value of the surface density of aptamer 1 by an independent methodology, this sequence was radiolabeled through reaction with γ-^{32}P-ATP and T4 polynucleotide kinase, which transferred a phosphate group to the 5′ position of the oligonucleotide. It was assumed that a small phosphate group should not interfere with the immobilization process. Then, immobilization of aptamer 1 was performed from exposure to a set of dilutions (0.055 – 55 μM). The number of molecules of aptamer 1 per cm^2, before and after MCH application, are summarized in Table 1. In all cases control experiments using an oligonucleotide sequence without phosphorothioate were performed to determine inespecific binding.

It can be remarked, that approximately 50% reduction of the immobilized aptamer on the surface was observed after MCH treatment, which is in agreement with the removal of oligonucleotide non-specific linkages [8]. Surface density values of phosphorothioate immobilization are also in agreement to reported thiol oligonucleotides anchoring cases [8, 11].

Table 1. Comparison of surface densities (in molecules per $cm^2 \times 10^{-11}$) obtained by independent experiments of immobilization of aptamer 1 and performance of the SAMs for recognition of radioactive γ-^{32}P-ATP by unlabeled aptamer 1.

[Apt 1] (μM)	Number of molecules ($cm^2 \times 10^{-11}$)		
	Oligonucleotide immobilized		ATP recognized
	Before MCH	After MCH	γ-^{32}P-ATP
0.055	7.4 ± 0.7	3.5 ± 0.4	0.28 ± 0.03
5.5	49 ± 5	20 ± 2	18 ± 2
40	200 ± 25	72 ± 7	17 ± 2
55	500 ± 50	280 ± 30	0.028 ± 0.003

In order to evaluate thermal stability of phosphorothioate anchoring, aptamer 1 and 2 sequences were immobilized on gold, and surface density was measured by chronocoulometric experiments in the presence of 50 μM $[Ru(NH_3)_6]^{3+}$. Then, both sequences were exposed to thermic stress by immersing the electrode for 20 minutes in 10mM Tris buffer (pH 7.4) at 80 °C and a new surface density measurement was done. In the case of the immobilization of aptamer 1, the number of molecules/cm^2 was reduced approximately 70% after heating, meanwhile thiol immobilized sequence (aptamer 2) diminished surface density in 60%. These results indicated a similar thermal stability between both sequences, which is an important issue taking into account necessary denaturalization process to potentially regenerate the recognition assembly.

Another important parameter to be explored is biosensor recognition performance as function of the oligonucleotide surface density. It is known that oligonucleotide packing density deeply affects the biosensor response [22], so to establish the oligonucleotide concentration that afforded the optimum surface coverage, aptamer 1 was immobilized from different solution concentrations over Au surfaces. Then, different immobilization experiments were incubated with γ-^{32}P-ATP, and the radioactive label was measured, expecting that the most appropriate oligonucleotide con-

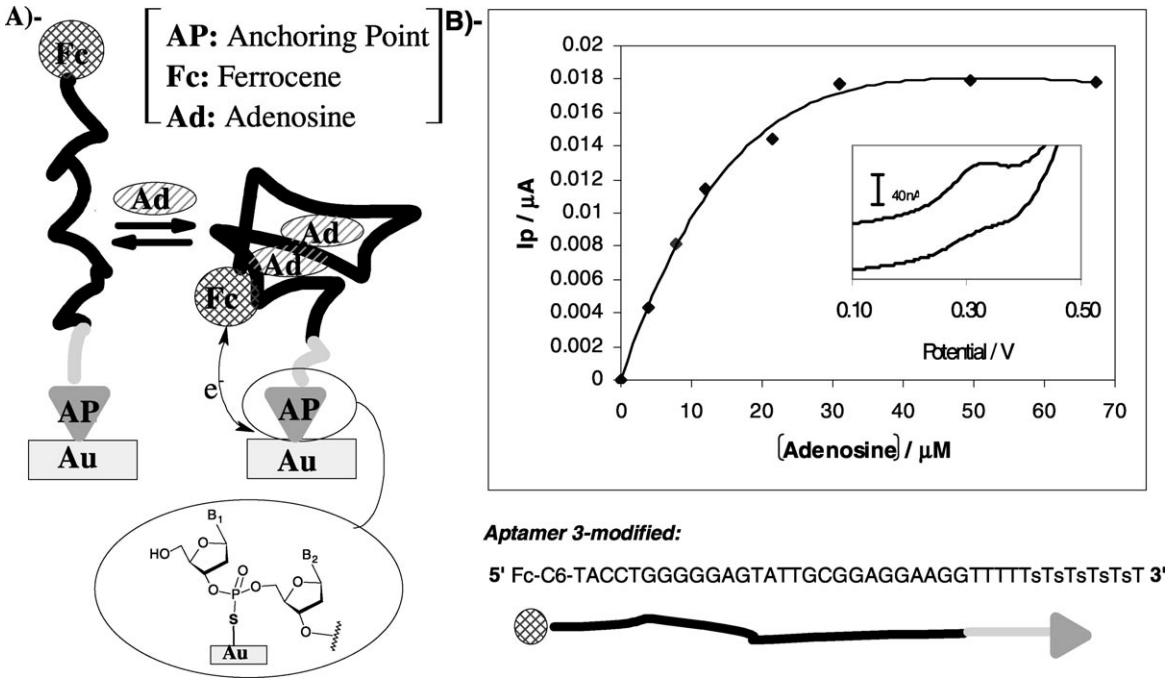

Fig. 2. A) Schematic representation of sensor architecture. B) Response curve of Aptamer 3 modified with ferrocene, as function of [Adenosine]/µM; inset: SWV of immobilized Aptamer 3 modified with ferrocene: no adenosine added (lower line), 50 µM adenosine (upper line).

centration captured the highest radiolabeled ATP. Data in Table 1 showed that ATP recognition depends on surface coverage and the best performance was reached when 5.5 µM aptamer 1 solution concentration was used, as indicated by the highest γ-^{32}P-ATP detected.

Having evaluated phosphorothioate and thiol linkages in relation to molecular surface density and thermal stability, aptamer 3 was used as a proof of concept of a phosphorothioate E-AB sensor. The binding of adenosine to the aptamer induces a folding transition from a random coil like conformation to a quite well defined structure [5], as represented in Figure 2A. This conformational rearrangement allows translation of the recognition event into an electrochemical response. Taking these facts into account, aptamer 3 sequence was assembled on the electrode and the *N*-hydroxysuccidimidyl ferrocene derivatization was done in situ. The electrode was rinsed with HEPES buffer several times and exposed to increasing concentrations of adenosine to prove its ability to recognize the specific target.

SWV was applied to measure ferrocene response observing a current increase as more adenosine was incorporated in the recognition layer (Fig. 2B). Ferrocene peak current (see Figure 2B, inset) for each adenosine concentration was registered (peak potential = 0.318 – 0.323 V vs. Ag/AgCl, 3 M KCl, aqueous), and used to construct a typical response curve (Fig. 2B). The immobilized aptamer K_d was estimated from the corresponding Scatchard graphic and its value ($K_d = 5 \pm 3$ µM, three measurements on three independent electrodes) is in accordance with previously reported data (6 ± 3 µM, [19]). Specificity of the sensor was checked by using 100 µM guanosine solution without significant electrochemical response.

As conclusion, we have compared oligonucleotide phosphorothiate and thiol linkages surface densities, finding that both groups have similar performance. An E-AB sensor for adenosine using phosphorothioate has been developed showing that aptamer behavior is functional with this kind of anchoring. Further work is in progress in our laboratory in order to fully characterize phosphorothioate-Au assembling.

Experimental

Reagents. Three desalted DNA sequences (Sigma-Genosys, USA) were used without further purification. The adenosine original aptamer sequence (5′-AC CTG GGG GAG TAT TGC GGA GGA AGG T-3′) was modified in either 3′, 5′ or both termini depending on the experiment:

Aptamer 1: 5′-TsTsTs TsTsT TTT T*AC CTG GGG GAG TAT TGC GGA GGA AGG T*-3′, where Ts represents a phosphorothioate at 5′ termini followed by five additional thymidines (T) as linkers. In italics is represented the adenosine aptamer.

Aptamer 2: 5′-CH_3–$(CH_2)_5$–S–S–$(CH_2)_6$-TTT TT*A CCT GGG GGA GTA TTG CGG AGG AAG GT*-3′ contained a disulfide sequence that was reduced prior to immobilization to produce a thiol group.

Aptamer 3: 5′-NH_2–$(CH_2)_6$-T*AC CTG GGG GAG TAT TGC GGA GGA AGG TTT* TTTs TsTsTs TsT-3′ had a 5′-NH_2–$(CH_2)_6$-modification. This position was used to incorporate a ferrocene group to produce an electroactive aptamer.

Mercaptohexanol (MCH) was purchased from Sigma Aldrich. All other chemicals were analytical grade and used as purchased. Water (18 MΩ cm^{-1}) was provided by a Millipore Simplicity equipment.

Instruments. Electrochemical experiments were performed in a standard three electrode cell with a gold disk electrode (1.6 mm diameter, Metrohm) as working electrode, a Ag/AgCl (3 M KCl, aqueous) as reference electrode and a Pt-wire as counter electrode. Cyclic voltammetry (CV), square wave voltammetry (SWV) and chronocoulometric experiments were carried out on an Autolab PGStat10 (EcoChemie) equipped with GPES v.4.9 software. Solutions were purged with N_2 (g) for 5 min before measurement.

SWV experimental conditions: Scan potential: −0.1 to 0.6 V, step potential: 0.0051 V, amplitude: 0.01995 V.

Radioactive ^{32}P labeling was quantified using a calibrated Liquid Scintillator Counter (Wallac 1214 Rackbeta Pharmacia) and a Storm 820 (Molecular Dynamics). In this case 1.0 cm × 0.5 cm gold plates were used.

Acknowledgement

This work is supported by ANPCyT (PICT 05:38348), CONICET (PIP 5462) and Universidad Nacional de General Sarmiento. J. M. M. is CONICET member. The authors thank Laura Robaldo for her assistance in radioactive labeling.

References

[1] I. Willner, M. Zayats, *Angew. Chem. Int. Ed.* **2007**, *46*, 6408.
[2] K. Navani, Yingfu Li, *Curr. Op. Chem. Biol.* **2006**, *10*, 1.
[3] M. Famulok, J. S. Hartig, G. Mayer, *Chem. Rev.* **2007**, *107*, 3715.
[4] R. Stoltenburg, C. Reinemann, B. Strehlitz, *Biomol. Eng.* **2007**, *27*, 381.
[5] C. H. Lin, D. J. Patel, *Chem. Biol.* **1997**, *4*, 817.
[6] I. Willner, M. Zayats, in *Aptamer in Bioanalysis* (Ed: M. Mascini), Wiley, New York **2009**, pp. 63–86, and references cited therein.
[7] J. C. Love, L. A. Estroff, J. K. Kriebel, R. G. Nuzzo, G. M. Whitesides, *Chem. Rev.* **2005**, *105*, 1103.
[8] T. M. Herne, M. J. Tarlov, *J. Am. Chem. Soc.* **1997**, *119*, 8916.
[9] R. Levicky, T. M. Herne, M. J. Tarlov, S. K. Satija, *J. Am. Chem. Soc.* **1998**, *120*, 9787.
[10] A. B. Steel, R. L. Levicky, M. J. Tarlov, *Biophys. J.* **2000**, *79*, 975.
[11] P. Gong, C.-H. Lee, L. J. Gamble, D. G. Castner, D. W. Grainger, *Anal. Chem.* **2006**, *78*, 3326.
[12] C.-Y. Lee, P. Gong, G. M. Harbers, D. W. Grainger, D. G. Castner, L. J. Gamble, *Anal. Chem.* **2006**, *78*, 3316.
[13] F. Eckstein, *Oligonucleotides and Analogs. A Practical Approach*, Oxford University Press, Oxford, New York **1991**.
[14] R. P. Iyer, W. Eagan, J. B. Reagan, S. L. Beaucage, *J. Am. Chem. Soc.* **1990**, *112*, 1253.
[15] T. Ihara, M. Nakayama, M. Murata, K. Nakano, M. Maeda, *Chem. Commun.* **1997**, 1609.
[16] H. Brisset, A.-E. Navarro, N. Spinelli, C. Chaix, B. Mandrand, *Biotechnol. J.* **2006**, *1*, 95.
[17] A. Kumar, S. Phadtare, R. Pasricha, P. Guga, K. N. Ganesh, M. Sastry, *Curr. Sci.* **2003**, *84*, 71.
[18] L. Jiang, H. Zhang, J. Zhuang, B. Yan, W. Yang, T. Li, C. Sung, *Adv. Mat.* **2005**, *17*, 2066.
[19] D. Huizenga, J. W. Szostak, *Biochem.* **1995**, *34*, 656.
[20] A. Steel, T. M. Herne, M. J. Tarlov, *Anal. Chem.* **1998**, *70*, 4670.
[21] N. Oyama, F. C. Anson, *Anal. Chem.* **1990**, *52*, 1192.
[22] R. C. White, N. Phares, A. A. Lubin, Y. Xiao, K. W. Plaxco, *Langmuir* **2008**, *24*, 10513.

